

Using magnetotelluric and seismic geophysical observations to infer viscosity for Glacial Isostatic Adjustment calculations

Ramirez, F.¹, Selway, K.², and Conrad, C.P.¹

¹ Centre for Earth Evolution and Dynamics, University of Oslo, Norway

² Department of Earth and Planetary Sciences, Macquarie University, Australia

Main idea: Lateral variations in mantle viscosity can be better constrained by utilizing both seismic and magnetotelluric geophysical measurements. Such constraints are needed for models of GIA deformation.

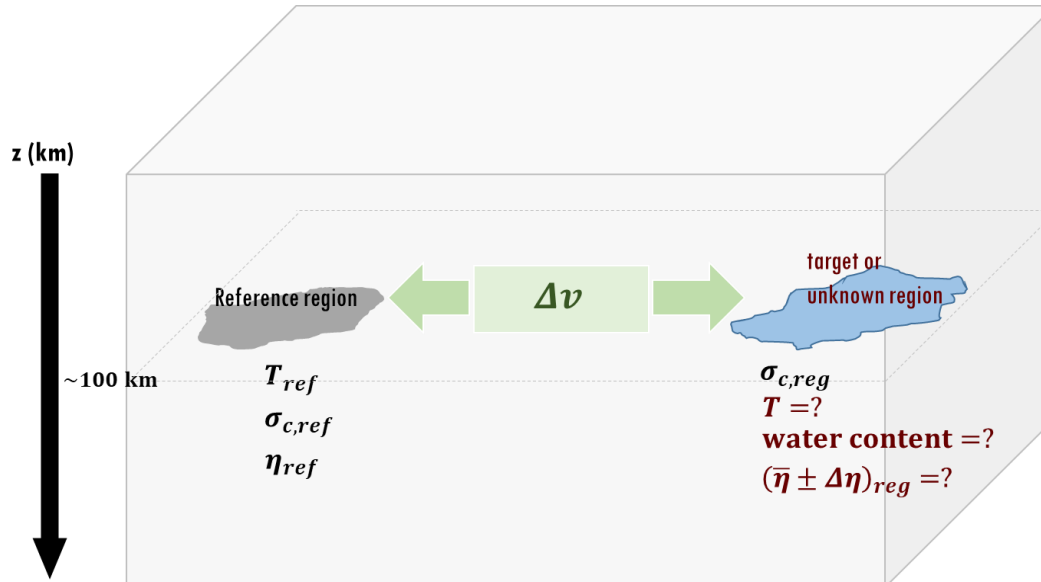


Figure 1. Mantle viscosity between a reference region (left) and an unknown target region at 100 km depth. We would like to constrain the viscosity ratio between these regions. Both regions are assumed to have the same differential stress of 0.1 MPa and grain size of 10 mm. We assume that the reference region has a reference temperature T_{ref} and electrical conductivity $\sigma_{c,ref}$ (from MT observations). The viscosity of the reference region η_{ref} can be calculated since temperature is assumed and the water content is known from MT. For a given velocity anomaly of Δv between the regions, we can infer the temperature of the target region. Combining this temperature with a water content (derived from the observed electrical conductivity $\sigma_{c,reg}$), viscosity of the target region can be calculated.

Mantle viscosity is an important Earth parameter because it controls a variety of processes including Glacial Isostatic Adjustment (GIA). Yet, mantle viscosity poorly constrained because we cannot measure it directly from geophysical observations. However, geophysical measurements such as magnetotellurics (MT) and seismics provide information on parameters (e.g., temperature and water content) that influence mantle viscosity. By constraining these parameters, the mantle viscosity calculation can also be constrained.

In this study, we investigate how MT and seismic data can constrain a lateral difference in mantle viscosity between a known reference region and an unknown target region. Consider a reference region (melt-free) at 100 km depth with reference temperature T_{ref} , electrical conductivity $\sigma_{c,ref}$ (from MT), and viscosity η_{ref} as seen in Figure 1. The η_{ref} can be calculated since reference temperature and water content are known at a given stress σ and grain size d , by using the strain rate equation (e.g., Hirth & Kohlstedt, 2003; Ohuchi et al, 2015)

$$\dot{\epsilon} = A\sigma^n d^{-p} f_w^r \exp\left(-\frac{E^* + PV^*}{RT}\right)$$

where $\eta = \sigma / \dot{\epsilon}$. From seismic tomography, we assume that observations of velocity anomalies Δv between a target region and a reference region result from a temperature difference between these regions. Given that this target region has a measured absolute conductivity of $\sigma_{c,reg}$ from MT, the water content (COH) can then be determined. Consequently, η for the target region can be calculated by using the constrained water content and T range. To visualize how viscosity can be constrained from T and water content, we illustrate (Figure 2) how viscosity varies according to parameters inferred from seismic and MT measurements, respectively.

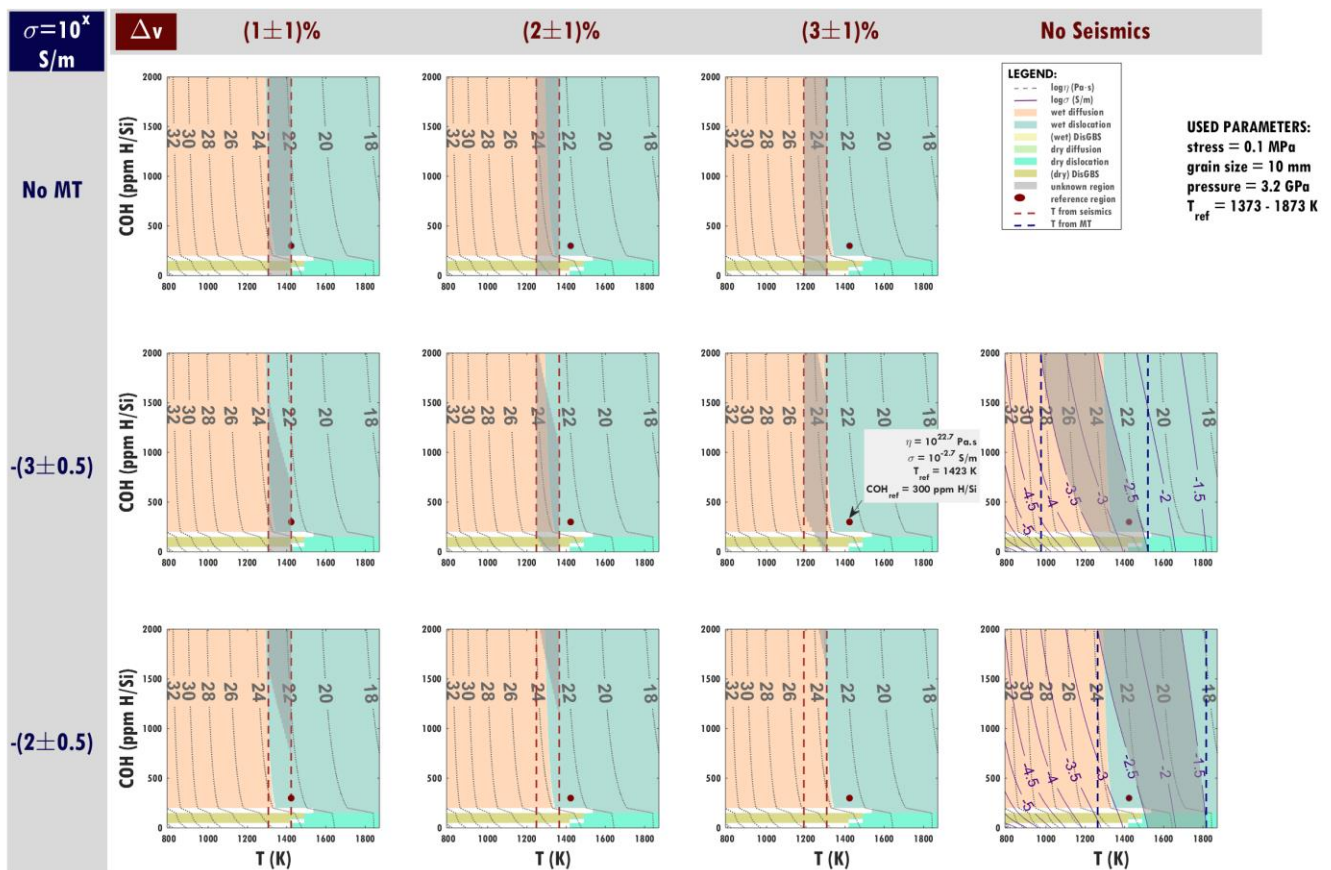


Figure 2. Example of viscosity and deformation mechanism maps for 100km depth, 0.1 MPa stress and 10 mm grain size. Shown is viscosity as a function of water content (COH, y-axes) and temperature (T, x-axes), for different combinations of seismic and MT data. The strain rates from the various deformation mechanisms (diffusion, dislocation and dislocation-accommodated grain-boundary sliding or DisGBS) for both dry (<150 ppm H/Si) and wet (>150 ppm H/Si) olivine aggregates are calculated using the flow law parameters used in Ohuchi et al. (2015). From the calculated (total) strain rates, (effective) viscosities are computed as indicated by the dashed grey contour lines. A reference region at 1423 K and 300 ppm H/Si is represented by a red dot, while the target region is represented by a grey patch. For a given velocity anomaly Δv (column in the figure) with respect to the reference region and absolute electrical conductivity σ (row in the figure), the viscosity range of the target region can be determined, and is better constrained if both seismic and MT data are available.

This viscosity map figure shows the reference region conditions as a red dot at a temperature of 1423 K and a COH of 300 ppm H/Si. The possible viscosity range of the target (or unknown) region is represented by a grey patch, for a given velocity anomaly compared to the reference region Δv (column in the figure) and electrical conductivity σ (row in the figure). The target and reference (red dot) regions are considered to have the same stress of 0.1 MPa, grain size of 10 mm and pressure of 3.2 GPa.

In the 'No MT' row, the target regions (rectangular grey patches) have temperature range colder than the reference region (in red dot) due to the positive Δv . Since water content is not constrained in 'No MT' case, the grey regions have 0 to 2000 ppm H/Si water content. From this, we can infer that the rectangular grey patches allow for relatively large viscosity ranges on the viscosity map.

In the 'No Seismics' column, the physical conditions of the unknown region are calculated only from MT data, with no seismic constraints. MT data are sensitive to both temperature and water content, so the resulting grey shaded region is a band sloping from high COH and lower temperatures to low COH and higher temperatures. Again, at the uncertainty levels modelled, these correspond to large viscosity ranges.

Next we combine these two geophysical measurements, as seen in the inner 6 panels. The grey patches become smaller, and thus viscosity becomes better constrained, because both temperature and water content are constrained by the combination of the seismic and MT measurements.

References

Hirth, G. and D.L. Kohlstedt (1996), Water in the oceanic upper mantle: Implications for rheology, melt extraction and the evolution of the lithosphere, *Earth Planet. Sci. Lett.*, 144, 93–108.

Hirth, G. and D.L. Kohlstedt (2003), Rheology of the Upper Mantle and the Mantle Wedge: A View from the Experimentalists, *Inside the Subduction Factory*, *Geophysical Monograph* 138, 83-105.

Keppler, H. and N. Bolfan-Casanova (2006), Thermodynamics of Water Solubility and Partitioning, *Rev. Mineralogy & Geochemistry*, 62, 193-230.

Ohuchi, T., et al. (2015), Dislocation-accommodated grain boundary sliding as the major deformation mechanism of olivine in Earth's upper mantle, *Sci. Adv.*, 1, e1500360.

Selway et al. (2019), Upper mantle melt distribution from petrologically constrained magnetotellurics, *Geochemistry, Geophysics, Geosystems*, 20, 3328-3346.

Warren, J. and G. Hirth (2012), Grain size sensitive deformation mechanisms in naturally deformed peridotites, *Earth & Planetary Sci. Lett.*, 248, 438-450.